

Measured aerodynamic forces on a full scale 2MW turbine in comparison with EllipSys3D and HAWC2 simulations

H Aa Madsen, N N Sørensen, C Bak, N Troldborg and G Pirrung

Technical University of Denmark, DTU Risøe Campus, Frederiksborgvej 399, DK 4000 Roskilde, Denmark

E-mail: hama@dtu.dk

Abstract. Design loads on turbines are normally simulated with an aeroelastic model using an engineering BEM type model with the turbulent inflow generated with a turbulence model like the Mann model. There are several fundamental uncertainties in this approach, e.g. how well the unsteady induction in response to the turbulent flow is computed. However, within the last few years full 3D CFD rotor computations with turbulent inflow have been performed which can provide detailed insight into this complex load response. In the present work we present computations with the EllipSys3D solver on the 80m diameter NM80 turbine used in the DANAERO project where surface pressure measurements at four radial positions were conducted. The aerodynamic loads integrated from the pressure distributions have been derived and compared with computations by the aeroelastic code HAWC2. Overall a very good correlation is found by comparing PSD spectra of the measured sectional blade forces with HAWC2 simulations using specific flow input from the meteorology mast at six heights. In another comparison using purely turbulent inflow for the simulations on the NM80 rotor some deviations between the force spectra are found between EllipSys3D results and HAWC2 simulations at the inboard part of the blade and at high frequencies.

1. Introduction

Detailed experimental data on the aerodynamics of full scale turbines are sparse and much of the aeroelastic code validation is therefore carried out comparing integral moments, torque and power. However, this is an uncertain way of validating codes as counteracting model deficiencies unintendedly can lead to a satisfactory correlation with experiments. Therefore detailed aerodynamic measurements on full scale turbines operating in the atmospheric flow are highly needed. Such type of measurements were carried out in 2009 within the DANAERO project [1],[2],[3]. Pressure distributions were measured at four radial stations on the full scale blade of the 80m diameter NM80 rotor. The unsteady aerodynamic loads integrated from the pressure distributions provide a unique basis for detailed validations of low fidelity codes like lifting line and BEM type codes using airfoil data as input. In the present work the validation exercise also comprises simulations with the EllipSys3D [5],[6] in a setup with turbulent inflow and a full resolution of the flow around the blades. Combining the high fidelity model results and the detailed experimental aerodynamic load response data form an ideal basis for the engineering model validation.

The low fidelity codes usually assume frozen turbulence, where the rotor is moved through a pregenerated turbulence box. We know however, that the flow is decelerated and expanding when approaching the rotor which means that the turbulent structures can be expected to be deformed to some degree. Also the details on how the induced velocities are computed for turbulent inflow and shear cannot directly be derived from the basic BEM theory as this is only valid for steady, uniform inflow. An improved insight into these questions and in general an investigation of the uncertainty of the aerodynamic load response in turbulent inflow are the main objective with the present model validation exercise.

Besides the detailed experimental aerodynamic data the high fidelity rotor computations by the EllipSys3D code provide an enhanced basis for engineering model validations as force and flow data can be extracted at almost arbitrary points which are not possible by the experimental data. The CFD simulations provide also insight into the requirements to the grid in order to resolve the atmospheric turbulent inflow and thus also the band width of the unsteady forces on the blades.

The paper is organized in the following way. A brief description of the DANAERO experiment and the approach for selecting the data set used in the present work are presented in section 2. Then follows a description of the modelling set-up for the HAWC2 and the EllipSys3D code in section 3. Finally, the comparisons and validation results are presented and discussed in section 4 followed by a conclusion section.

2. The DANAERO experiment and data selection for the present work

2.1. The DANAERO experiments

The DANAERO experiments were conducted in the period from 2007-2010 in cooperation between the Technical University of Denmark and the industrial partners Siemens, Vestas, LM and DONG Energy [1],[2]. The overall objective of the project was to provide detailed experimental data from full scale turbines in order to study fundamental aspects of aerodynamics, aeroelasticity and aeroacoustics. In a follow up DANAEROII project [3] from 2010-2013 the experimental data were processed and calibrated and finally stored in a data base.

2.2. Pressure and inflow measurements on the NM80 turbine

The main experiment in the DANAERO project was blade surface pressure and inflow measurements at four radial positions, approximately at $r/R=0.33$ (section 03), 0.48 (section 05), 0.75 (section 08) and 0.93 (section 10) on the NM80 turbine, see sketch to the left in Figure 1 and Table 1. section 10 of the blade. In order to install the surface pressure measurement equipment and the surface microphones it was necessary to build a completely new blade so that the instruments could be installed during the blade manufacturing process. This was in particular true for the two outboard instrumented sections as these sections could not be accessed after the blade assembling. The test blade installed on the turbine is shown on the photo to the right in Figure 1.

An overview of the blade instrumentation is given in Table 1. It comprised 64 pressure taps at four radial stations, five hole pitot tubes close to these radial positions and finally at the outboard section 56 flush mounted surface microphones.

Data acquisition was carried out with three different systems as the different type of sensors require different scan rates, Table 1. A common synchronization signal was sampled by all the three systems which allowed time alignment of the signals when postprocessing the data.

2.3. Selection of the data set for the present study

As the main objective of the present study has been to study the aerodynamic response in turbulent inflow we have searched for data sets where the wind shear is minimal, the rotational speed almost constant and no major yaw error. One particular test case with a length of 250 s

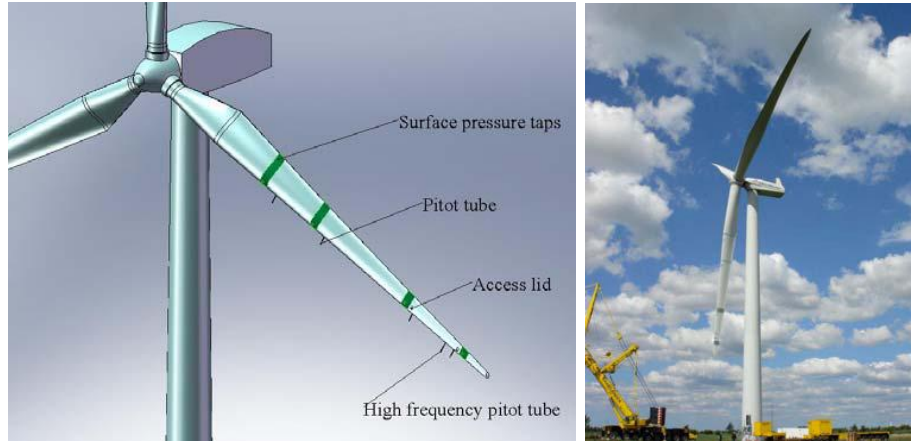


Figure 1: Left: Sketch showing an overview of the instrumentation of the test blade. Right: The test blade after installation on the turbine in May 2009, replacing one of the original blades.

Table 1: Instrumentation on the LM38.8 blade and data acquisition.

Instrument	Sensor	Position [m]	Sampling rate [Hz]
Strain gauges	Flapwise and edgewise moments	{3.0, 8.0, 13.0, 16.0, 19.0, 22.0, 26.0, 30.0, 34.0, 37.0}	35
Five-hole Pitot tubes	Relative velocity and flow angles	{14.5, 20.3, 31.0, 36.0}	35
Pressure taps	Surface pressure	{13.0, 19.0, 30.0, 37.0}	100
Accelerometers	Acceleration	{13.0, 19.0, 30.0, 37.0}	35
Thermometer	Blade temperature	{13.0, 19.0, 30.0, 37.0}	35
Microphones	Surface pressure	37.0	50000

from the DANAERO data base with a mean wind speed around 6m/s fulfilled these conditions as shown in Figure 2. The aerodynamic sectional forces for the case are shown in Figure 3. Finally the statistics of the main channels of the test case are presented in Table 2.

3. The set-up for HAWC2 and EllipSys3D simulations

It was decided to use only the HAWC2 simulations for direct comparison with the experimental data. This is mainly because there are minor differences in wind speed and wind direction over the span of the rotor as can be seen in Table 2 although the data set was chosen due to low wind shear. As these small deviations from uniform inflow were not included in the EllipSys3D simulations it causes an uncertainty in a direct comparison with the measurements. In HAWC2 the wind shear and veer were accounted for by adjusting the mean axial and cross wind speed as function of height. However, we make then a separate comparison between EllipSys3D and HAWC2 simulations for only turbulent inflow where the turbulence box for HAWC2 is generated from sampling of the CFD generated flow at the rotor position, however without the turbine inserted into the flow.

3.1. HAWC2 set-up for direct comparison with measurements

The mean wind speed at hub height of 57m is 6.04m/s with a Std dev of 0.41m/s as seen in Table 2. In HAWC2 the inflow mean speed was adjusted to the actual measured ones at the

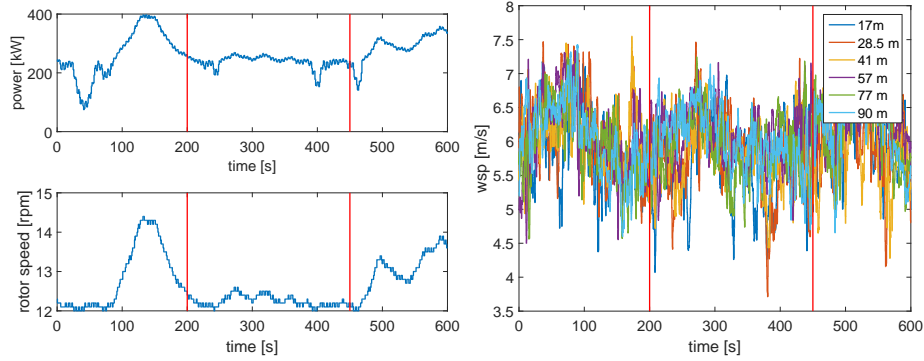


Figure 2: The 250 sec data set was chosen because as seen in the left figure, indicated between the red lines, the rotor speed is almost constant and close to 12 rpm. In the right figure the wind speed at six heights measured in the nearby meteorology mast indicate that the wind shear is low.

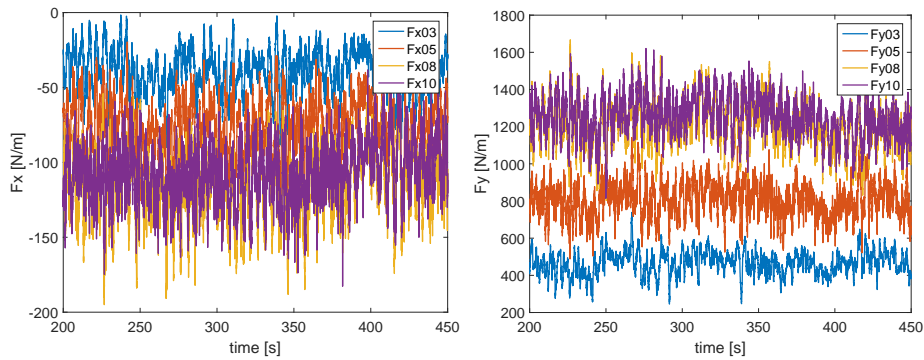


Figure 3: The aerodynamic sectional forces f_x , f_y in direction chordwise and perpendicular to the chord, respectively, integrated from the measured pressure distributions.

different heights shown in Table 2. Likewise a cross component wind speed is inserted to give the actual wind direction deviations from the wind direction at hub height.

A Mann [10] turbulence box was generated to fit the measured Std dev and mean wind speed at hub height. The following parameters were used: $\alpha\epsilon=0.014$, $L=33.9$, $\Gamma=3.9$ and seed nr. 34.
 Length of box : 1525m - resolution D_x : 0.37m N_x :4096
 Width of box : 81.92m - resolution D_y : 1.28m N_y :64
 Height of box : 81.92m - resolution D_z : 1.28m N_z :64

The box dimension in the flow direction fits the simulation time and the mean wind speed so that the entire box is used for the 250 sec simulation time. In the lateral direction the size of the box just encompasses the rotor. The seed was arbitrarily chosen to 34 but it will be shown later how the results vary for different seeds. In the left graph of Figure 4 a time trace of the axial flow component at the center of the Mann box is compared with the anemometer and sonic measurements at hub height. In the right graph the power spectra of the simulated wind show very good correlation with the anemometer spectrum.

Both simulations with the standard HAWC2 version with BEM aerodynamics as well as the version with a near wake model for the trailed vorticity HAWC2-NW [4] has been used for comparisons with the measurements. The rotor speed was constant and set to the measured

	Unit	Mean	Std.dev	Min	Max
Wind speed at 17m	[m/s]	5.73	0.58	4.07	6.98
Wind speed at 28.5m	[m/s]	5.79	0.54	3.71	7.46
Wind speed at 41m	[m/s]	5.81	0.48	4.43	7.06
Wind speed at 57m	[m/s]	6.04	0.41	4.84	7.16
Wind speed at 77m	[m/s]	5.94	0.44	4.74	7.25
Wind speed at 93m	[m/s]	6.00	0.45	4.70	7.14
Wind dir at 17m	[deg]	232.30	7.32	201.77	257.16
Wind dir at 57m	[deg]	228.09	6.01	201.39	245.07
Wind dir at 93m	[deg]	232.75	5.73	213.75	265.45
Yaw position	[deg]	228.97	0.00	228.96	228.97
Yaw error	[deg]	0.89	6.01	-16.10	27.58
Fx03	[N/m]	39	14	2	90
Fx05	[N/m]	75	19	20	147
Fx08	[N/m]	115	23	53	195
Fx10	[N/m]	107	19	35	183
Fy03	[N/m]	466	64	245	739
Fy05	[N/m]	805	90	488	1142
Fy08	[N/m]	1217	121	802	1667
Fy10	[N/m]	1253	110	814	1621
Power	[kW]	238.7	20.0	153.0	269.0
Rotation speed	[rpm]	12.3	0.1	12.0	12.6
Pitch	[deg]	0.18	0.06	0.15	0.30
Density	[kg/m ³]	1.23	0.00	1.22	1.23

Table 2: The statistics of the main channels for the selected data set.

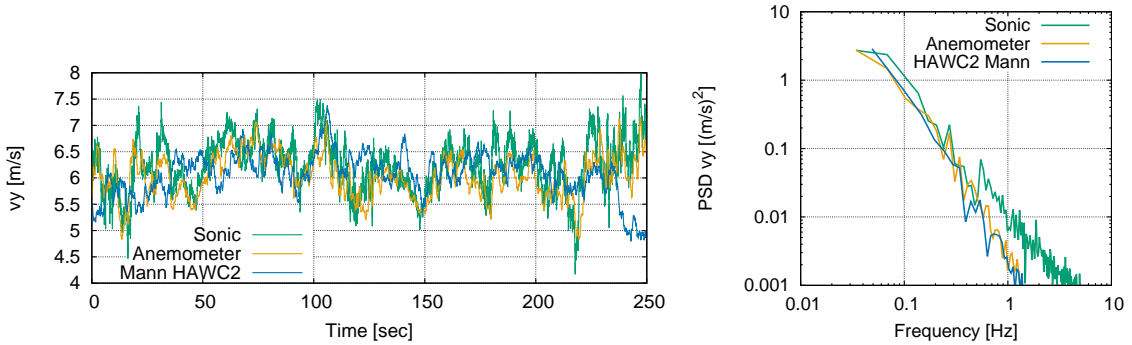


Figure 4: The wind speed variation and the PSD of the velocity component in the flow direction in the center of the Mann box in comparison with time variation and PSD of the hub height anemometer and sonic measurement.

value of 12.3 rpm as seen in Table 2. The airfoil data set used is based on 2D wind tunnel tests on four airfoil sections with the same geometry as the sections on the rotor. A 3D correction was afterwards applied using the 3D correction model of Bak [7]. Further information on the airfoil data set can be found in [8].

3.2. The set-up of the *EllipSys3D* simulations

A comprehensive work on rotor simulations with turbulent inflow was conducted within the recently finished project AVATAR.EU. This work is reported in [9] and contains a detailed

description of the grid set-up used for the EllipSys3D simulations on the AVATAR and NM80 rotor. Therefore only a brief description is enclosed here.

The in-house flow solver EllipSys3D is used for the CFD rotor simulations [5] [6]. An overset grid setup is used for the computations. The rotor is positioned centrally 500 [m] downstream of the inlet plane in the background stretched Cartesian grid. The Cartesian grid region covers 2000 x 2000 x 1500 [m³] using 384 x 384 x 320 cells in the two cross-flow directions and along the flow direction. A region of cubic cells, 2 x 2 x 2 [m³] is positioned from the inlet plane and reaching 600 meters into the domain, spanning an area of 200 x 200 [m²] in the crossflow plane. Outside of the constant region the grid is stretched towards the far-field.

The rotor grid is a curvilinear O-O-topology with 256 cells around the rotor blades in the chord-wise direction, 129 cells in the span-wise direction and 64 cells in the normal direction. The cell size in the wall normal direction is 1×10^{-6} [m] assuring a y^+ value below 2 and extending 15 [m] away from the blade surfaces. To bridge the region between the background grid and the curvilinear grid around the rotor geometry an intermediate cylindrical domain is used. The radius of the cylindrical domain is 80 meters and the axial extend is +/- 12 meters, in total it holds 2.8 million grid points. The total number of cells in the grid used for the computations is equal to 33 million cells. Boundary conditions: At the upstream inlet plane, the velocities are dynamically updated according to the transient Mann turbulence files. At the down-stream outlet plane a fully developed flow assumption is applied. At the four cross flow planes, inlet conditions are specified according to the mean flow quantities. At the rotor blade surface, a no-slip condition is applied.

The Mann turbulence box used for the turbulence generation in the CFD simulations has the following parameters: $\alpha\epsilon=0.014$, $L=33.60$, $\Gamma=3.9$ and seed nr. 34.

Length of box : 2048m - resolution Dx : 2.00m - Nx :1024

Width of box : 512m - resolution Dy : 2.00m - Ny : 256

Height of box : 512m - resolution Dz : 2.00m - Nz : 256

Comparing this box with the previous presented one for the aeroelastic simulations it has a lower resolution but still with the double resolution of what was used in the CFD simulation comparisons in the AVATAR project on the AVATAR rotor [9]. The EllipSys3D simulations using the Mann box were carried out two times. One with the rotor inserted. Another one without the rotor where the turbulence velocity components were sampled at the position of the rotor on a square area around the rotor with the dimension of 128x128 [m²] and a resolution of 1 [m] in the rotor plane (vertical and horizontal) and 2 [m] in the flow direction. This turbulence was then used in the HAWC2 simulations for direct comparison with the EllipSys3D code.

4. Results

4.1. HAWC2 simulations compared with measurements

A comparison of the spectra of the measured and simulated force components, tangential and normal to the chord, respectively, are shown in Figure 5 and 6. A very good correlation is found, however with slightly lower spectra in the simulations at the highest frequencies for the two outboard sections. The increasing influence of the rotational sampling, shifting energy of the spectrum below 1p to higher frequencies, is clearly seen in the comparison of the spectra at the different radial positions. It can also be seen that the difference between the two versions of HAWC2 is small when comparing these spectra. Further it can be noted that we tested the influence of a coarser turbulence grid with a resolution of 2.94 x 2.56 x 2.56 [m³] and found a considerably lower correlation with the measurements, particularly lower peaks at 1p, 2p etc..

A comparison of the Std dev of the simulated and measured unsteady aerodynamic forces along the blade is shown in Figure 7. For the chordwise component the correlation is almost perfect while there is a tendency to an underestimation of the Std dev on the outboard part of the blade and the opposite on the inboard part. When comparing the results from the two

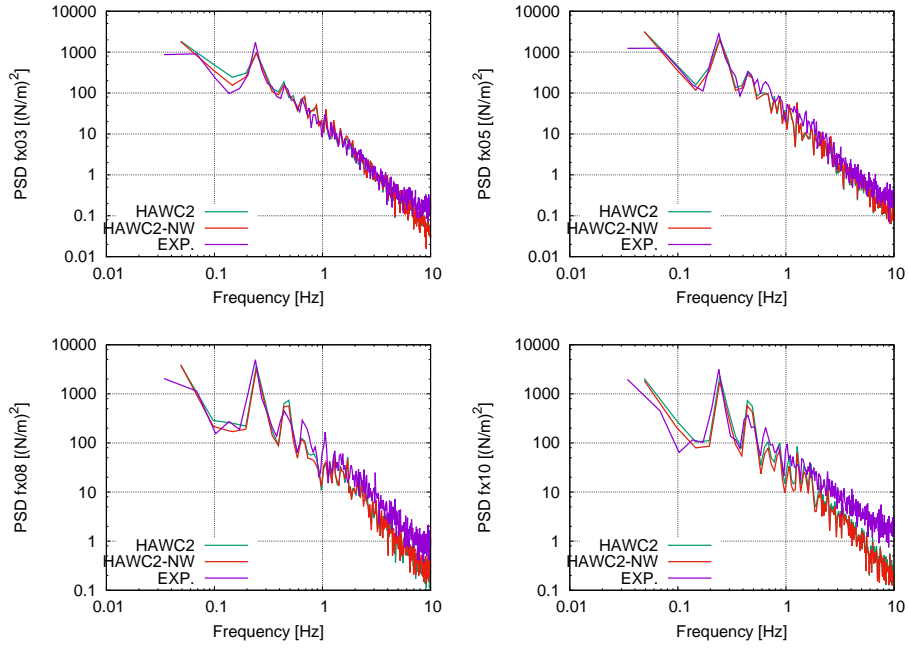


Figure 5: Spectra of the chordwise force component simulated with the HAWC2 and HAWC2-NW code, respectively, in comparison with spectra of the measured forces.

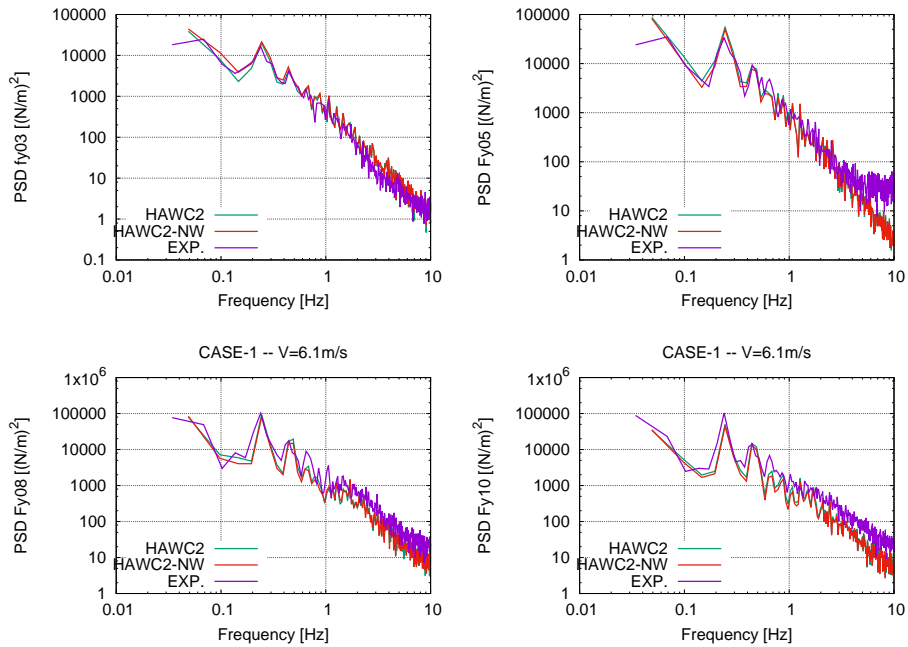


Figure 6: Spectra of the normal to chord force component simulated with the HAWC2 and HAWC2-NW code, respectively, in comparison with spectra of the measured forces.

versions of the HAWC2 code the slightly lower Std dev predicted with HAWC2-NW is expected as the increased dynamic induction in that model counteract the unsteady turbulent inflow

components at the blade.

The tendency mentioned above with slightly under prediction of the Std dev of the unsteady forces on the outboard part and the opposite on the inboard part is also apparent in Figure 8 where the accumulated power spectra of the normal force component as function of frequency are shown for different seeds of the turbulence used in the HAWC2 simulations. For the two outboard sections the increased accumulated energy is not least found at the highest frequencies. It corresponds to the small deviations found in the spectra above. As concerns the differences in spectra between the different seeds much are due to differences at the lowest frequencies as expected due to the high statistical uncertainty here. If the spectra were shifted to the same value at e.g. 0.1 Hz the deviations at higher frequencies would be much less.

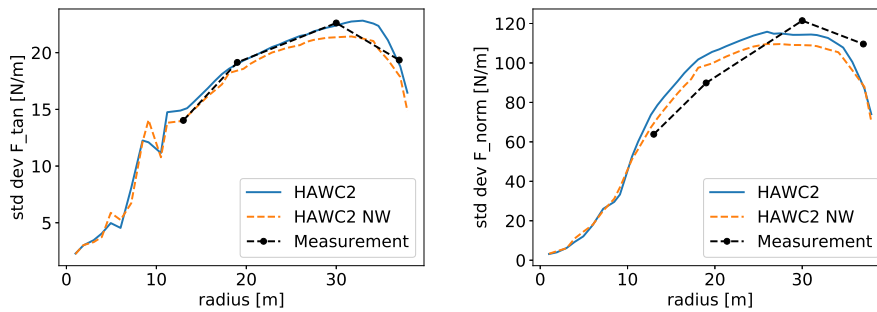


Figure 7: Std. dev. along the blade span of the unsteady aerodynamic force component tangential and normal to the chord, respectively, simulated with the HAWC2 and HAWC2-NW code and measured ones.

4.2. A comparison of *EllipSys3D* and *HAWC2* simulations

Using the turbulence field sampled from the CFD generated flow field as input for the HAWC2 simulations provides an optimal basis for a detailed comparison as the uncertainty of differences in flow input is reduced to a minimum. We use the spectra of the in-plane (IP) and out-of-plane (OOP) aerodynamic forces for comparison of the models, Figures 9 and 10. For the outboard two sections the spectra for the OOP forces correlate well as seen in Figure 10. However, for all the sections the spectra of the CFD simulations start to decrease above 2-3 Hz which is not seen in the HAWC2 simulations. The reason for this tendency is not clear and will be further investigated. For the most inboard section the results deviate due to stall in the CFD simulations and this influences also partly the results at the neighboring section. The stall is not seen in the measured pressure distributions and not in the HAWC2 simulations so this discrepancy is another subject for further investigations.

5. Conclusions

A data set comprising aerodynamic sectional forces at four radial positions derived from blade pressure measurements on a full scale rotor has been compared with results from the aeroelastic HAWC2 code with BEM type aerodynamics. A very good correlation of spectra of the forces is found with only minor tendencies to deviations. This indicates that the many assumptions and simplifications in simulating the force response to turbulent inflow in a BEM type engineering aeroelastic code do not cause major uncertainty in the simulated loads. This is confirmed by a parallel comparison with simulated aerodynamic forces with the high fidelity *EllipSys3D* code for the two outboard sections at 75% and 93% radial position although deviations are seen in

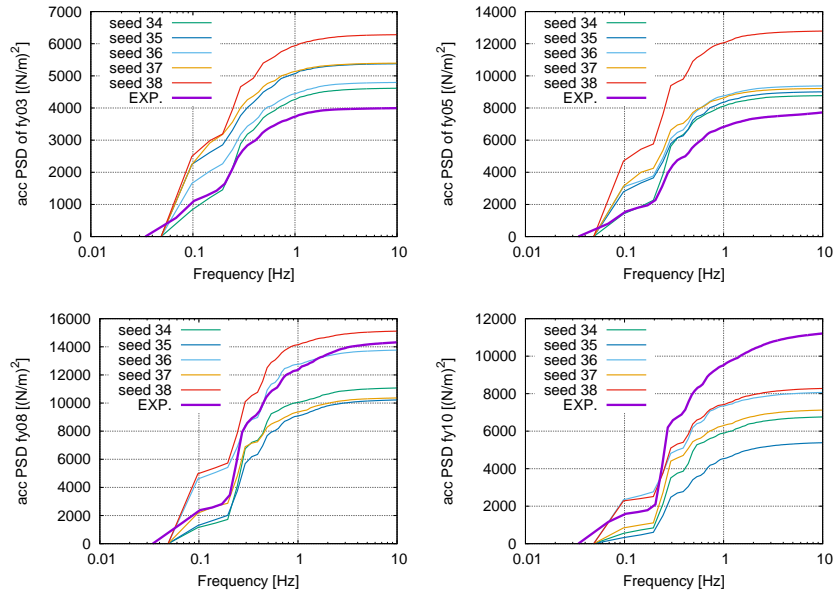


Figure 8: Accumulated spectra of the normal to chord force component simulated with the HAWC2 code for different seed numbers in the turbulence generation and compared with accumulated spectra of the measured forces.

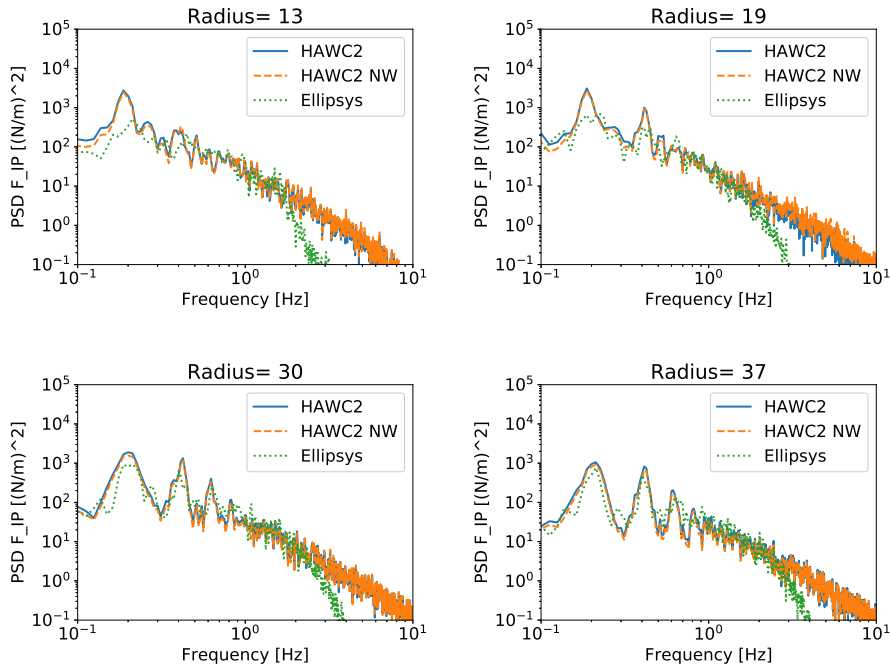


Figure 9: Spectra of the inplane force component simulated with the EllipSys3D code in comparison with HAWC2 and HAWC2-NW simulations.

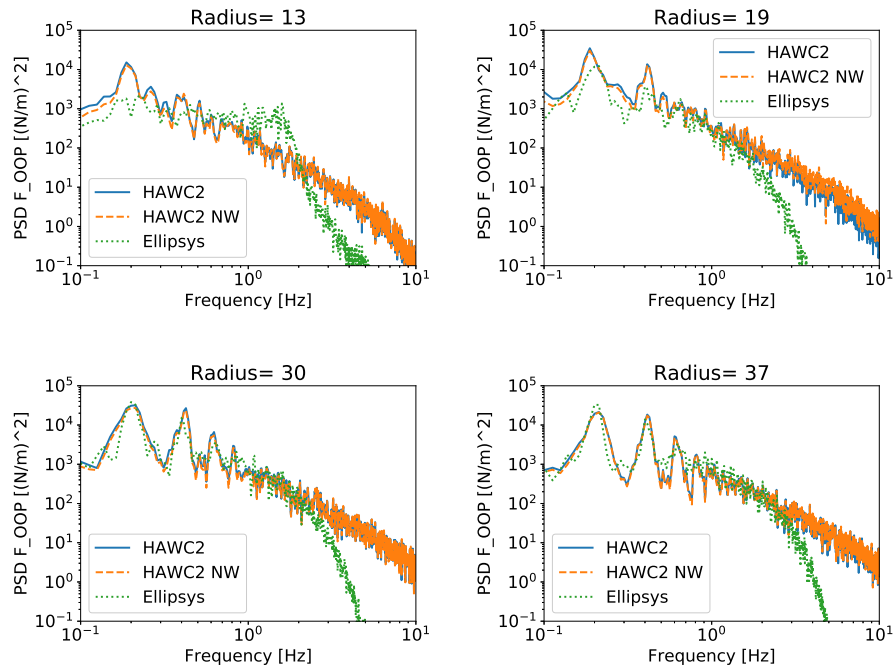


Figure 10: Spectra of the out of plane force component simulated with the EllipSys3D code in comparison with HAWC2 and HAWC2-NW simulations.

the spectra for frequencies above 2-3 Hz. For the two inboard stations major deviations were found due to stall in the CFD simulations which was not seen in the HAWC2 simulations and not in the measured pressure distributions. This will be further investigated.

References

- [1] Madsen H Aa, Bak C, Schmidt US, Gaunaa M, Fuglsang P, Romblad J, Olesen NA, Enevoldsen P, Laursen J and Jensen L, 2010. The DANAERO MW Experiments. Danmarks Tekniske Universitet, Risø Nationallaboratoriet for Bredlygtig Energi.
- [2] Madsen H Aa, Bak C, Paulsen US, Gaunaa M, Sørensen NN, Fuglsang P, Romblad J, et al. 2010. The DANAERO MW Experiments. 48th Aiaa Aerospace Sciences Meeting Including the New Horizons Forum and Aerospace Exposition, 20100645.shdshsd
- [3] Troldborg N, Bak C, Madsen H Aa and Witold R (2013). DANAERO MW: Final Report. DTU Wind Energy.
- [4] G. R. Pirrung, H. Aa. Madsen, T. Kim, and J. Heinz. A coupled near and far wake model for wind turbine aerodynamics. *Wind Energy*, 19(11):2053-2069, 2016.
- [5] Michelsen JA. Basis3D- a platform for development of multiblock PDE solvers. Technical Report AFM 92-05, Technical University of Denmark, Department of Fluid Mechanics, 1992.
- [6] Sørensen NN. General purpose flow solver applied to flow over Hills. Technical Report Risø-R- 827-(EN), Risø National Laboratory, Roskilde Denmark, 1995.
- [7] Bak, C., Johansen, J. and Andersen, P.B. Three-Dimensional Corrections of Airfoil Characteristics Based on Pressure Distributions. Presented at the European Wind Energy Conference and Exhibition (EWEC), February 27 to March 2, 2006, Athens, Greece
- [8] Madsen et. al, Validation of advanced models against measured data. Aerodynamics of Large Rotors - WP2, Deliverable 4.2, AVATAR.EU.
- [9] Yusik et al., Effects of inflow turbulence on large wind turbines. AVATAR Deliverable D2.5, AVATAR.EU.
- [10] Mann J. The spatial structure of neutral atmospheric surface-layer turbulence. *J. Fluid Mech.*, 273:141168, 1994.